linewidths of both the p states and the s states are very narrow, (generally <0.1 Å), and as a result both states are well resolved.

Another interesting observation is the apparent quenching of the hole spin. One expects the hole spin to be anisitropic ($g_h = g_{h||}\cos\theta$; see Fig. 2). The contribution of the hole spin should be observed for the orientation $C||H$. The experimental results of the energy values as a function of the angle θ between the magnetic-field direction and the z axis are given in Fig. 5. The energies are for the $n=2$ states of the I_{8a} and I_{8b} donors given in Table I and in Fig. 3. One observes little dependence on the angle θ; also, the multiplicity is accounted for at all angles including $\theta=0$ by the orbital and spin splittings of the $n=2$ state electrons. The same experimental results are shown in Fig. 6 for the I_{9a} and I_{9b} complexes of Table I and Fig. 4.

IV. CONCLUSIONS

The study of excited states of bound exciton complexes is a very useful tool for gaining information about impurity states in semiconductors. We have shown that after exciton decay from a bound neutral donor complex the donor electron is left in an excited state in a number of transitions in CdSe. From the energies of the transitions one can determine the donor binding energies. Studying the same excited states in a magnetic field has yielded information concerning the effective mass of the electron.

In the case of CdSe, as well as CdS, excited terminal states were observed only for donor complexes. In CdSe a contribution from the hole spin in the upper state was not observed. This leads to the conclusion that the hole g value in these bound complexes is very small.

PHYSICAL REVIEW VOLUME 177, NUMBER 3 15 JANUARY 1969

Schottky Barriers on GaAs*

M. F. Millea and M. McColl
Aerospace Corporation, El Segundo, California 90045

AND

C. A. Mead
California Institute of Technology, Pasadena, California 91109

(Received 16 September 1968)

The forward current of Schottky barriers on n-type GaAs is investigated as a function of electron concentration in the range of 8×10^{17} to 8×10^{18} cm^{-3} at temperatures 297–4.2°K. Both vacuum-cleaved and chemically polished surfaces are used. The majority of the junctions studied are gold Schottky barriers, but tin and lead contacts are also examined. The predominant current mechanism is field emission at liquid-nitrogen temperature and below for the range of electron concentrations used. These data are in excellent quantitative agreement at 77°K with the field-emission analysis of Padovani and Stratton if one uses a two-band model for the imaginary wave number k_n. At 297°K, thermionic field emission predominates, but for an electron density above 3×10^{18} cm^{-3} the field-emission mechanism with a two-band model still gives reasonable agreement.

I. INTRODUCTION

With the introduction of quantum mechanics, various attempts were made to apply it to physical phenomena that were thus far unexplained. One such effort was an attempt to explain the rectification behavior of metal-semiconductor contacts. Various models[1–3] were purposed which assumed that the mechanism of electron flow was tunneling through a potential barrier that existed at a metal-semiconductor interface. This model was rejected because, among other things, it predicted the wrong direction of rectification.[4,5] Thermionic-emission models that postulated the thermal excitation of electrons over a potential barrier were successful in explaining the main experimental feature of rectification as of that early stage.[6,7] Bethe[8] considered a thermionic-emission mechanism to explain the forward characteristic of silicon point contacts used as mixers. He showed that with this model one would expect the slope of the natural logarithm of the current as a function of applied voltage to be

* Work supported by the U. S. Air Force under Contract No. F04695-67-C-0158.

[1] A. H. Wilson, Proc. Roy. Soc. (London), **A136**, 487 (1932).
[2] L. Nordheim, Z. Physik **75**, 434 (1932).
[3] J. Frenkel and A. Joffé, Physik. Z. Sowjetunion **1**, 60 (1932).
[4] N. F. Mott and R. W. Gurney, *Electronic Processes in Ionic Crystals* (Oxford University Press, London, 1940).
[5] H. K. Henisch, *Rectifying Semiconductor Contacts* (Oxford University Press, London, 1957).
[6] N. F. Mott, Proc. Roy. Soc. (London), **A171**, 281 (1939); **A171**, 27 (1939).
[7] W. Schottky, Z. Physik **113**, 367 (1939); **118**, 539 (1942).
[8] H. A. Bethe, MIT Radiation Laboratory Report No. 43/12, 1942 (unpublished).

40 V^{-1} at 300°K, whereas a slope of 25 V^{-1} was observed with point contacts made on heavily doped silicon. Bethe proposed that this discrepancy might be a result of quantum-mechanical tunneling that permits thermally excited electrons to go through the surface barrier even though their energy is less than the barrier height (i.e., thermionic field emission).

The splendid work of Padovani and Stratton[9] rekindled interest in the rectifying behavior of metal-semiconductor contacts and brought a unifying analysis to the problem by indicating three regions of interest—thermionic emission, thermionic field emission, and field emission. Their analysis of thermionic field emission was compared with experimental results on an appropriately doped metal-GaAs junction, and reasonable agreement with the experimental semilog slope of the current-voltage characteristic as a function of temperature was obtained. In another paper, Padovani and Stratton[10] extended their analysis of the field emission and derived an expression that allows one to determine the pure imaginary electron wave vector in the forbidden gap. Investigations of metal-semiconductor contacts in the field-emission region have also been considered by other authors.[11–13]

In the work reported here the forward characteristics of metal contacts on heavily doped n-type gallium arsenide are investigated in the range where tunneling is the major mechanism of current flow. It is shown that Padovani and Stratton's treatment is in excellent agreement with these results, provided one uses a two-band model for the imaginary wave vector of the tunneling electrons and includes the contribution of the free electrons to the total space-charge density.

II. THEORY

In this section we present expressions for the forward current characteristics of Schottky barriers at a sufficiently low temperature that the electron flow occurs by field emission. This analysis follows the treatment by Padovani and Stratton[9,10] and the extension provided by Conley and Mahan.[11] The symbols used in this analysis are defined in Table I.

An illustration of the potential barrier of an n-type semiconductor-metal interface is shown in Fig. 1. At a sufficiently low temperature, the forward-current density J can be estimated[10,11] by just considering the electrons near the Fermi level:

$$J=J_m\exp\left(-\frac{S_m}{\alpha}\int_0^{E_B-E}\frac{k_n(\eta)d\eta}{(\eta+\frac{3}{5}\mu_F)^{1/2}}\right), \quad (1a)$$

TABLE I. List of important symbols.

J	Current density
E	Applied voltage-potential energy
E_B	Barrier height
E_g	Energy gap
k	Boltzmann's constant
k_n	Imaginary wave number of electron normal to barrier
m^*	Electron effective mass
N	Electron concentration
q	Electronic charge
T	Temperature (°K)
ϵ	Permittivity of semiconductor
μ_F	Fermi level degeneracy
$\hbar$	$(\frac{1}{2}\pi)\times$Planck's constant

where η is the energy of a tunneling electron at the semiconductor Fermi level with respect to the bottom of the conduction band;

$$\eta=V(z)-\mu_F. \quad (1b)$$

For a constant electron-tunneling mass equal to the free-electron effective mass (i.e., single-band model), one has

$$k_n(\eta)=\alpha\eta^{1/2}, \quad (1c)$$

where

$$\alpha=2(2m^*)^{1/2}/\hbar. \quad (1d)$$

Franz's[14–17] expression for the wave number of the electron for a two-band model is

$$k_n(\eta)=\alpha[\eta(E_g-\eta)/E_g]^{1/2}. \quad (1e)$$

The pre-exponential factor in Eq. (1a) is

$$J_m=\frac{A}{(c_1kT)^2}\frac{\pi c_1kT}{\sin(\pi c_1kT)}, \quad (1f)$$

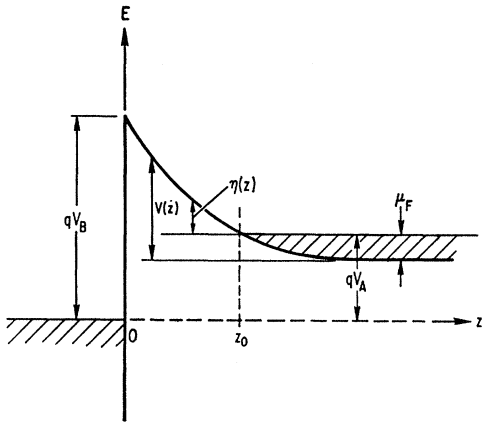

FIG. 1. Electron potential-energy diagram of a forward biased Schottky barrier.

[9] F. A. Padovani and R. Stratton, Solid-State Electron. **9**, 695 (1966).
[10] F. A. Padovani and R. Stratton, Phys. Rev. Letters **16**, 1202 (1966).
[11] J. W. Conley and G. D. Mahan, Phys. Rev. **161**, 681 (1967).
[12] J. W. Conley, C. B. Duke, G. D. Mahan, and J. J. Tiemann, Phys. Rev. **150**, 466 (1966).
[13] J. W. Conley and J. J. Tiemann, J. Appl. Phys. **38**, 2880 (1967).
[14] W. Franz, in *Handbuch der Physik*, edited by S. Flügge (Springer-Verlag, Berlin, 1956), Vol. XVIII, p. 155.
[15] E. O. Kane, J. Phys. Chem. Solids **1**, 249 (1957).
[16] C. M. Chaves, N. Majlis, and M. Cardona, Solid State Commun. **4**, 631 (1966).
[17] G. Lewicki and C. A. Mead, Phys. Rev. Letters **16**, 939 (1966).

where

$$A=m^*q(kT)^2/2\pi^2\hbar^3 \tag{1g}$$

and

$$c_1=\tfrac{1}{2}S_m\ln\left(\frac{4(E_B-E)}{\frac{3}{5}\mu_F}\right). \tag{1h}$$

Although the quantity c_1 was calculated for the single-band model,[18] it is essentially the same for the two-band model. The quantity S_M is

$$S_m=\frac{2}{q\hbar}\left(\frac{\epsilon m^*}{N}\right)^{1/2}. \tag{1i}$$

Referring to Fig. 1, in the region $Z>Z_0$ where the Fermi level is in the conduction band, the space-charge potential needed in Eq. (1b) is not parabolic with distance, as it is when the Fermi level is below the conduction band. Conley and Mahan[11] show that an excellent over-all approximation for the space-charge potential for degenerate material is

$$V(z)=\frac{q^2N}{2\epsilon}(Z-Z_1)^2+\tfrac{2}{5}\mu_F, \tag{1j}$$

where

$$Z_1=\left[\frac{2\epsilon}{q^2N}(E_B-E+\tfrac{3}{5}\mu_F)\right]^{1/2}. \tag{1k}$$

For the single-band model, Eq. (1a) integrates to

$$J=J_m\exp\left\{-S_m\left[(E_B-E)^{1/2}(E_B+\tfrac{3}{5}\mu_F-E)^{1/2}-\tfrac{3}{5}\mu_F\ln\left(\frac{(E_B-E)^{1/2}+(E_B+\tfrac{3}{5}\mu_F-E)^{1/2}}{(\frac{3}{5}\mu_F)^{1/2}}\right)\right]\right\}, \tag{2}$$

while for the two-band model, it integrates to

$$J=J_m\exp\left\{-\tfrac{2}{3}S_m\left(\frac{E_g+\frac{3}{5}\mu_F}{E_g}\right)^{1/2}\times\left[[E_g+(6/5)\mu_F]\mathcal{E}(\chi,P)-(6/5)\mu_F\mathfrak{F}(\chi,P)-(E_g+\tfrac{3}{5}\mu_F-E_B+E)\times\left(\frac{(E_B-E)(E_g-E_B+E)}{(E_B+\tfrac{3}{5}\mu_F-E)(E_g+\tfrac{3}{5}\mu_F)}\right)^{1/2}\right]\right\}, \tag{3}$$

where

$$\sin\chi=\left(\frac{(E_g+\tfrac{3}{5}\mu_F)(E_B-E)}{E_g(E_B+\tfrac{3}{5}\mu_F-E)}\right)^{1/2},$$

$$p=[E_g/(E_g+\tfrac{3}{5}\mu_F)]^{1/2},$$

and $\mathfrak{F}(X,P)$ and $\mathcal{E}(X,P)$ are incomplete elliptic integrals of the first and second kind, respectively.

[18] R. Stratton, J. Phys. Chem. Solids **23**, 1177 (1962).

An expression particularly useful in analyzing tunneling results is obtained by differentiating $\ln J$ with respect to the applied voltage potential energy.[10,11] Neglecting the weak voltage dependence of J_m, the following expression is obtained:

$$k_n^2(\eta)\,|_{\eta=E_B-E}=\alpha^2(E_B-E+\tfrac{3}{5}\mu_F)(S/S_m)^2, \tag{4}$$

where

$$S=d(\ln J)/dE.$$

III. EXPERIMENTAL PROCEDURE

All Schottky barriers reported in this paper were formed on n-type GaAs obtained as (111) wafers from either Monsanto or Bell and Howell. These commercial houses furnished the appropriate electron concentration and mobility as determined from Hall-effect measurements. Both pulled and boat-grown crystals were employed, and no difference between surface barrier contacts formed on the two types of material was observed.

Schottky barriers were evaporated on both vacuum cleaved and chemically polished surfaces. For vacuum-cleaved junctions, rods were sectioned from the GaAs wafer perpendicular to a (110) cleavage plane. Tin-alloyed low-resistance contacts were formed at the ends of these rods, after which they were chemically cleaned. The rods were subsequently cleaved in vacuum in an evaporating stream of gold.[19] Contacts were isolated in good cleavage areas by scribing.

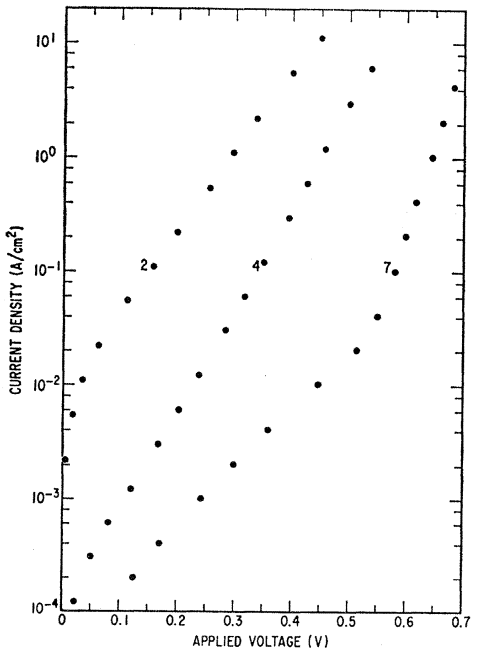

FIG. 2. Forward-current characteristics of Au-GaAs vacuum-cleaved Schottky barriers at 77°K.

[19] R. J. Archer and M. M. Atalla, Ann. N. Y. Acad. Sci. **101**, 697 (1963).

All Schottky barriers on chemically polished surfaces were evaporated on As(111) faces. A selected section of a wafer was tin alloyed to a Kovar tab, mechanically polished, and chemically polished in methanol +5% (by volume) bromine for 4 min. The surface was then exposed to an HF vapor and quickly inserted into an evaporating chamber. Metal masks were used to define the contacts. Gold, tin, and lead contacts were fabricated on chemically polished surfaces.

The capacitance was determined with a Boonton Model 74 C-S8 capacitance bridge. The current-voltage measurements were performed with an Autodata digital voltmeter and a Hewlett-Packard Model 412A vacuum-tube voltmeter when only 2% accuracy in current readings were required. When an accuracy of

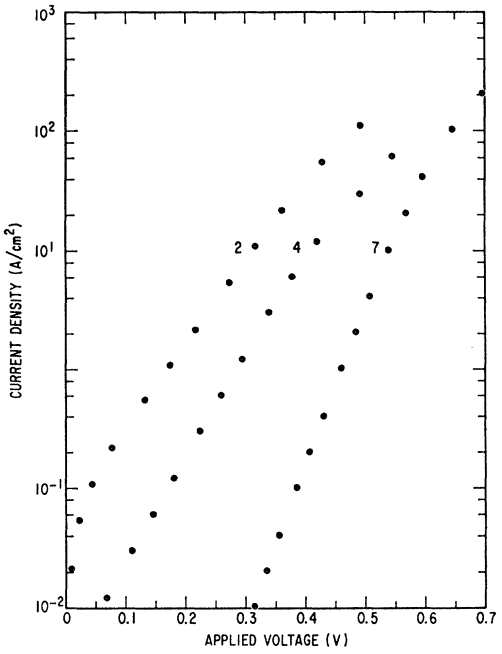

FIG. 3. Forward-current characteristics at 297°K of the same junctions presented in Fig. 2.

better than $\frac{1}{10}$% on current measurements was required, a precision resistor-digital voltmeter was also used as the ammeter.

IV. EXPERIMENTAL RESULTS

The current-voltage characteristics of gold contacts on three vacuum cleaved GaAs specimens with different electron concentrations are shown in Figs. 2 and 3 for temperatures of 77 and 297°K, respectively. The forward-current behavior of contacts evaporated on chemically polished surfaces is shown in Figs. 4 and 5. (These devices were made from the same material used to fabricate the junctions of Figs. 2 and 3.) Unit designations idenfifying the individual diodes are indicated in these figures. The electron concentration

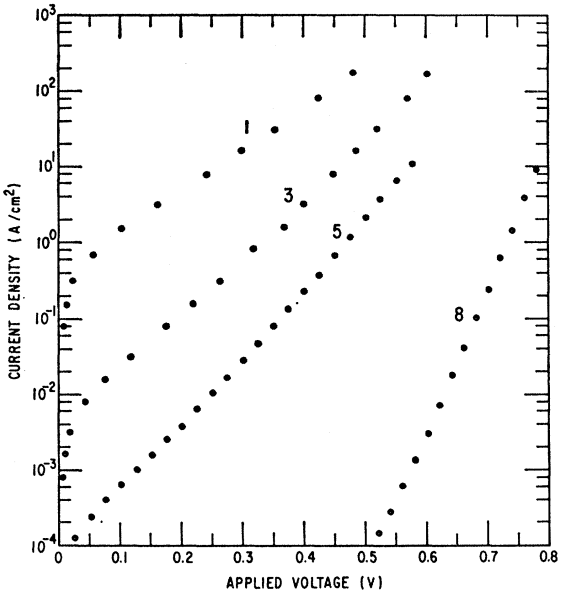

FIG. 4. Forward-current characteristics of Au-GaAs chemically polished Schottky barriers at 77°K.

determined by the Hall effect and the surface preparation of the eight gold-GaAs surface barriers discussed in this paper are listed in Table II. No intrinsic difference is observed between Schottky barriers on vacuum-cleaved surfaces and chemically polished surfaces prepared in the manner described. This applies to both the *I-V* and the capacitance-voltage dependence, and it insures that our chemically polished Schottky barriers have no appreciable interfacial layer between the metal and the GaAs.

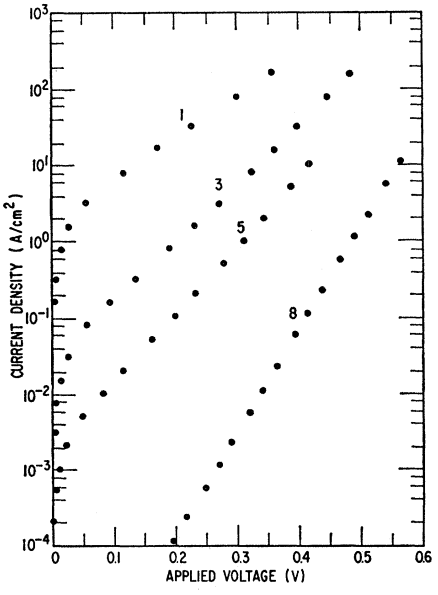

FIG. 5. Forward-current characteristics at 297°K of the same junctions presented in Fig. 4.

TABLE II. Surface preparation of Schottky barriers, and manufacturer's Hall-effect measurement of electron concentration.

Junction	Electron concentration (cm^{-3})	Surface preparation
1	8.0×10^{18}	Chemically polished
2	4.8×10^{18}	Vacuum cleaved
3	4.8×10^{18}	Chemically polished
4	2.5×10^{18}	Vacuum cleaved
5	2.5×10^{18}	Chemically polished
6	2.5×10^{18}	Chemically polished
7	8.0×10^{17}	Vacuum cleaved
8	8.0×10^{17}	Chemically polished

Two minor differences between vacuum-cleaved and chemically polished devices were noticed. As one can see from Figs. 2–5, the vacuum-cleaved junctions have a higher series resistance than the chemically polished junctions. This difference can be accounted for by the location of the back contacts. Also, both vacuum-cleaved and chemically polished devices have leakage at the edge of the metal contacts. This leakage is more pronounced with lower electron concentration, at lower voltages, and lower temperatures. It is more pronounced on vacuum-cleaved than on chemically polished barriers. The leakage current on vacuum-cleaved surfaces results from GaAs damage introduced during the scribing procedure used to define the contact area. Chemically etching vacuum-cleaved Schottky barriers removes the scribing damage and decreases the leakage. Unfortunately, chemical etching also changes the electrical properties of the barriers in a manner which suggests that a thin interfacial layer was introduced between the metal and the GaAs surface by the etching procedure.

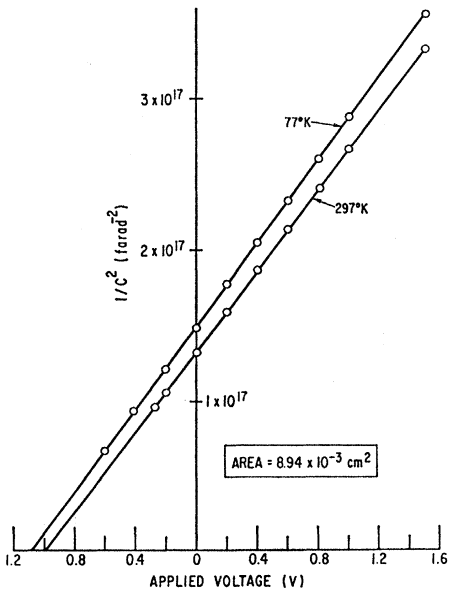

FIG. 6. Capacitance-voltage dependence of junction 8 at 77 and 297°K.

Whenever possible the electron concentration and barrier height were determined from the capacitance-voltage measurements. A typical plot of $1/C^2$ versus applied voltage is shown in Fig. 6. These data are from a chemically polished surface barrier (junction 8 of Figs. 4 and 5). The change in slope between 297 and 77°K suggests a decrease of either the dielectric constant or carrier density of approximately 2% from its room-temperature value. Using a value of 12.5 for the dielectric constant one would estimate, following the analysis of Conley and Mahan,[11] a carrier concentration of 1.0×10^{18} cm^{-3} and a barrier height of 1.03 eV at 77°K. The manufacturer's quoted electron concentration for this material is 8×10^{17} cm^{-3}. On all junctions examined that yielded reliable $1/C^2$-versus-V plots, the value of the barrier height ranged from 0.97 to 1.05 eV at 77°K. The chemically polished junctions in general exhibited slightly higher (perhaps 50 meV) barrier energy than vacuum-cleaved samples but in other respects gave identical results. A barrier height of 1.03 eV at 77°K will be used in the remainder of this paper for gold-GaAs junctions.

The electron concentration calculated from the capacitance on vacuum-cleaved junctions is less accurate than for chemically polished structures because the area measurement is not as accurate as when a metal mask is used to define the junction.

With increasing doping it becomes difficult to obtain meaningful capacitance results because the shunt conductance increases greatly. The capacitance bridge used does not function with a shunt conductance higher than one millimho. It was necessary to use Hall-effect measurements to determine electron concentration at levels greater than 3×10^{18} cm^{-3}. This estimate is less accurate than that given by the capacitance data since it yields a weighted average of the carrier density over a large area of the wafer. Several experiments were performed to determine the uniformity of the concentration. In one such experiment, gold contacts were spaced over a complete wafer whose density was estimated by the Hall effect to be 8×10^{17} cm^{-3}. A profile of the concentration determined from the capacitance-voltage behavior showed a uniform increase from the center to the edge by 30%. The electron concentration determined from capacitance in the center of the wafter corresponded closely to the Hall-effect value. The current-voltage curves also change in a uniform manner from center to edge in agreement with the capacitance data.

This experiment was repeated on a wafer whose Hall-effect carrier density was 4.8×10^{18} cm^{-3}. Because of the high concentration, no capacitance results were obtained. When examining contacts, going from the center to the edge, the current at a given voltage increased in a manner that suggested an electron concentration 20% higher near the edge.

The semilog slope [i.e., $d(\ln J)/dE=S$] of the curves in Fig. 5 is shown as a function of applied voltage in

Fig. 7. The expected dependence of S on applied bias for the single-band model can be determined by combining Eq. (1c) and Eq. (4),

$$S=S_m\left(\frac{E_B-E}{E_B-E+\frac{3}{5}\mu_F}\right)^{1/2}, \quad (5)$$

and for the two-band model by combining Eq. (1d) with Eq. (4),

$$S=S_m\left(\frac{(E_B-E)(E_g-E_B+E)}{E_g(E_B-E+\frac{3}{5}\mu_F)}\right)^{1/2}. \quad (6)$$

Inspection of these two equations shows that the single-band model predicts a monotonic decrease in S with increasing bias, whereas the two-band model predicts an increase in S with applied forward voltage until near the flat-band condition (i.e., $E_B-E=\mu_F$). The experimental dependence of S on applied voltage follows the dependence expected from the two-band model.

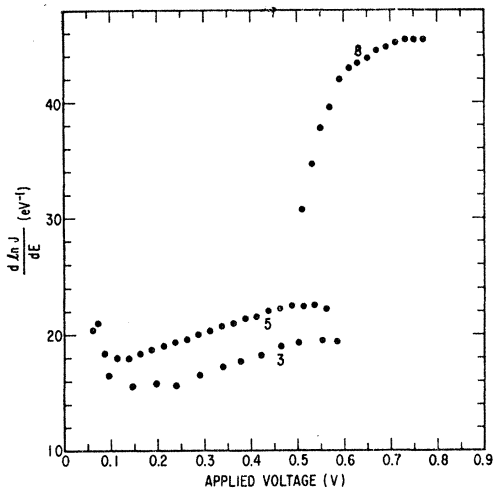

FIG. 7. Semilog slope of Schottky barriers at 77°K as a function of applied voltage.

For comparing the experimental results with the expected behavior when one uses a two-band model, it is convenient to rearrange Eq. (6) to

$$\frac{(E_B-E)(E_g-E_B+E)}{E_g}=(E_B-E+\tfrac{3}{5}\mu_F)\left(\frac{S}{S_m}\right)^2. \quad (7)$$

The left side of this equation is equal to $\alpha^{-2}k_n^2$. It should be emphasized that all the parameters in Eq. (7) are independently measurable. The left side of Eq. (7) is shown in Fig. 8 as the solid curve. The experimental results of junctions 5 and 8 are used to calculate the right side of Eq. (7) and are also presented in Fig. 8. The values listed in Table III are used in these calculations. The barrier height and electron concentration of junction 8 were determined from the capacitance-voltage dependence (see Fig. 6). The zero-bias capacitance of junction 5 is used to calculate the electron concentration with an assumed barrier height of 1.03 eV. The effective mass is known to depend on doping. An effective mass ratio of 0.076 is used in order to be consistent with Ukhanov and Mal'tsev's determination of this value by Faraday rotation is similarly doped GaAs.[20,21]

TABLE III. Values used in Eq. (7) to calculate $\alpha^{-2}k_m^2$ in Fig. 8.

E_g =	1.52eV
E_B =	1.03 eV
ϵ =	$12.5\epsilon_0$
m^* =	0.076×electron mass
N =	3.2×10^{18} cm^{-3} (junction 5)
N =	1.0×10^{18} cm^{-3} (junction 8).

An analysis similar to that discussed above was also performed for junction 3. Because of the high doping level of this sample (Hall-effect electron concentration indicated $N=4.8\times10^{18}$ cm^{-3}), no capacitance measurement could be obtained. An electron concentration of 4×10^{18} cm^{-3} had to be assumed for junction 3 to achieve agreement with the two-band model. As previously discussed, a variation of 20% in the electron concentration from the value determined by Hall effect is reasonable.

It is also interesting to compare the experimentally determined magnitude of forward current with the theoretical value. One method of accomplishing this is to select an arbitrary but convenient current density J_C and plot $\log_{10}J_0$, defined as $\log_{10}J_C-SE_A/\ln10$ versus S for samples of different carrier concentrations. Here E_A is the potential energy associated with the applied voltage of a particular junction needed to

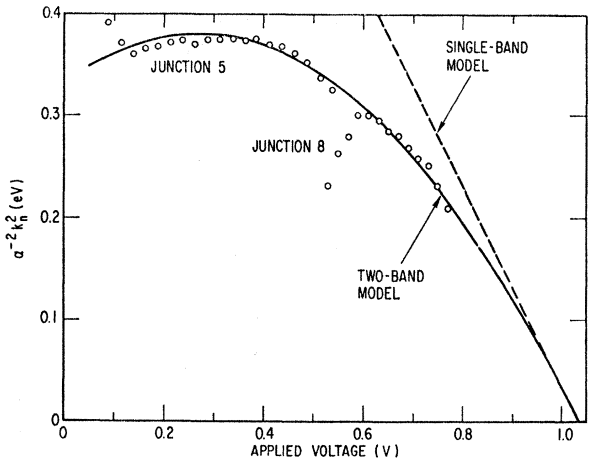

FIG. 8. Comparison of Franz's two-band model and the experimentally determined normallized imaginary electron wave vector.

[20] Yu. I. Ukhanov, Fiz. Tverd. Tela 5, 108 (1963) [English transl.: Soviet Phys.—Solid State 5, 75 (1963)].

[21] Yu. I. Ukhanov and Yu. V. Mal'tsev, Fiz. Tverd. Tela 5, 2926 (1963) [English transl.: Soviet Phys.—Solid State 5, 2144 (1964)].

achieve a current density of J_C. This is equivalent to assuming that $J=J_0 e^{SE}$ over a limited voltage range and experimentally determining J_0 versus S on junctions with different electron concentration at a given current density J_C. This has been done for our 77°K results at a current density of 1.0 A/cm², and the results are shown in Fig. 9. The datum point labeled PS-1 is taken from Padovani and Stratton.[10]

The theoretical dependence of $\log_{10}J_0$ on S for the two-band model is calculated from Eq. (3) for assumed barrier heights of 1.0 and 1.1 eV. The other constants needed for this calculation were taken from Table III. A similar calculation was performed for the single-band model using Eq. (2) and is plotted as the dashed curve in Fig. 9. It can be seen that reasonable agreement would be achieved between the two-band model and the present results for a barrier height of 1.03 eV.

The dependence of current on temperature, such as can be seen in Figs. 2–5, can be readily explained by the temperature variation of the barrier energy and the presence of thermionic field emission at 297°K, especially with the lower-doped Schottky barriers. One estimates from Fig. 6 that the barrier height is lowered from 1.03 eV at liquid-nitrogen temperature to 0.95 eV at room temperature; this change is typical for both vacuum-cleaved and chemically polished surfaces and nearly equal to the variation of forbidden gap with temperature. This barrier lowering results in an increase in current with increasing temperature. The fraction of thermionic field emission relative to field emission also increases with temperature and barrier thickness (i.e., inversely with electron density). Padovani and Stratton[9] have presented a detailed analysis of thermionic field emission for a single-band model.

The theoretical conditions that have been defined[9] for field emission are very stringent. At 77°K, these conditions are fulfilled for the type of Schottky barriers studied here above an electron density of 7.6×10^{17} cm^{-3} and, therefore, for all junctions we investigated. A doping above 8×10^{18} cm^{-3} is required at 297°K to fulfill the field-emission condition. Even though this condition is not fulfilled for the heavily doped specimens studied here, the field-emission expression will be shown to be reasonably accurate at room temperature for concentrations above 3×10^{18} cm^{-3}.

The change in the exponential forward region with temperature for the more heavily doped units (1–5) can be reasonably characterized by assuming that field emission is the predominant mechanism at both 77 and 297°K and by considering only the temperature dependence of the barrier energy. Below 3×10^{18} cm^{-3}, thermionic-field emission must be considered. Schottky barriers formed on specimens with a doping less than 3×10^{18} cm^{-3} (units 6–8) show a much larger variation

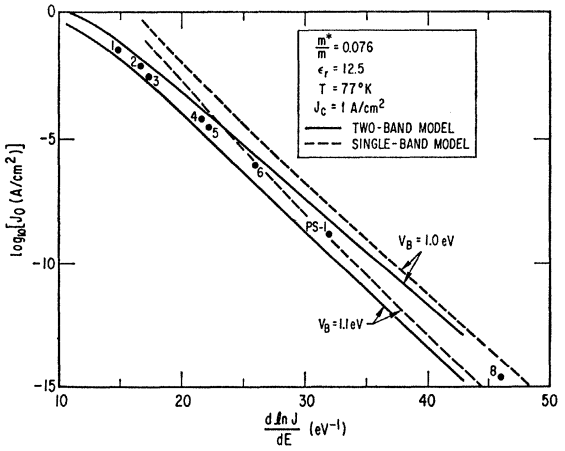

FIG. 9. Experimentally determined $\log_{10}J_0$ versus $d\ln J/dE$ at 77°K evaluated at a current density of 1.0 A/cm². The calculated dependence for the two-band model (solid curves) and single-band model (dashed curves) for 1.0- and 1.1-eV barrier energies are indicated.

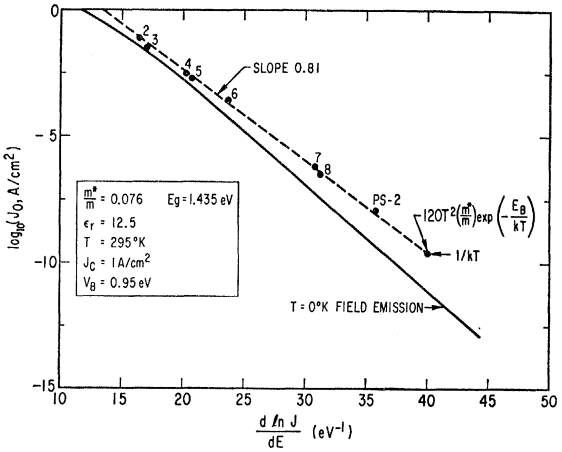

FIG. 10. Experimentally determined $\log_{10}J_0$ versus $d\ln J/dE$ at 297°K evaluated at 1.0 A/cm². The solid curve is the calculated 0°K field-emission dependence. The calculated thermionic-emission value is also indicated along with the experimental result obtained from Ref. 9.

in current with temperature because not only does the barrier decrease with increasing temperature but the current flow is well into the thermionic-field-emission region at room temperature.

The experimental room-temperature current-voltage behavior of junction 8 can be represented as

$$J=4\times10^{-7}\,e^{30.4E}\ \text{A/cm}^2.$$

Using the electron concentration of 1.0×10^{18} cm^{-3} (calculated from Fig. 6), the barrier height of 0.95 eV, and the effective-mass ratio of 0.076 one estimates, according to Padovani and Stratton's analysis of thermionic field emission (including Conley and Mahan's correction to the space charge), that

$$J=1\times10^{-7}\,e^{33.4E}\ \text{A/cm}^2,$$

which is in reasonable agreement with the experi-

mentally determinated dependence. The fact that the calculated pre-exponential factor is lower and the semi-log slope is higher than the experimentally determined values is to be expected since Padovani and Stratton's analysis assumes a single-band model for the tunneling electrons.

A plot of $\log_{10}J_0$ versus S at a constant current density of 1.0 A/cm² for the room-temperature results is presented in Fig. 10. The data for junction 1 are not included in this presentation because at a current density of 1.0 A/cm² the exponential region of the volt-ampere dependence is not sufficiently developed (i.e., the electron flow from metal to semiconductor is comparable to the forward-current flow). At a current density of 10 A/cm², junction 1 is in the exponential region and it is estimated that $\log_{10}J_0=0.29$ and $S=12.4$ V^{-1}. The datum point designated PS-2 is taken from Padovani and Stratton,[9] who state an electron concentration of approximately 5×10^{17} cm^{-3} for this Au-GaAs contact.

If the predominant current flow occurred by thermionic emission (i.e., thermal excitation of carrier over the barrier), one would expect that[5]

$$J=120T^2(m^*/m)e^{-(E_B-E)/kT}\quad \text{A/cm}^2.$$

The $\log_{10}J_0$ and S expected from thermionic emission calculated from this equation, using $E_B=0.95$ eV and $m^*/m=0.076$, is included in Fig. 10. The theoretical $\log_{10}J_0$-versus-S dependence for field emission at 0°K with $E_B=0.95$ eV is also included. In this calculation the room-temperature energy gap at 1.435 eV is used along with the room-temperature Fermi level.

A simple relation is observed for the experimental results in Fig. 10,

$$J_0=10^5e^{0.81S}\quad \text{A/cm}^2.$$

It can also be observed that the value for thermionic emission falls on this line. This relation is, of course, only valid for a current density of 1.0 A/cm². The more heavily doped Schottky barriers are in reasonable agreement with the 0°K field-emission curve. Deviation from the theoretical 0°K field-emission curve occurs at an electron concentration of approximately 3×10^{18} cm^{-3}.

Although gold Schottky barriers received the major effort because of their high barrier heights and stability, other metals have been used. After a preliminary study of various metals, tin and lead were selected for detailed measurements because these contacts have barrier energies that are significantly different from that of gold. The current-voltage behavior of a tin contact on a chemically polished surface made from the same ingot as junctions 7 and 8 is presented in Fig. 11. The capacitance dependence reproduced in Fig. 12 indicates a carrier concentration of 8.2×10^{17} cm^{-3} and a barrier height of 0.83 eV at liquid-nitrogen temperature. This barrier height is typical for tin contacts. Using the above values in Eq. (3), along with other

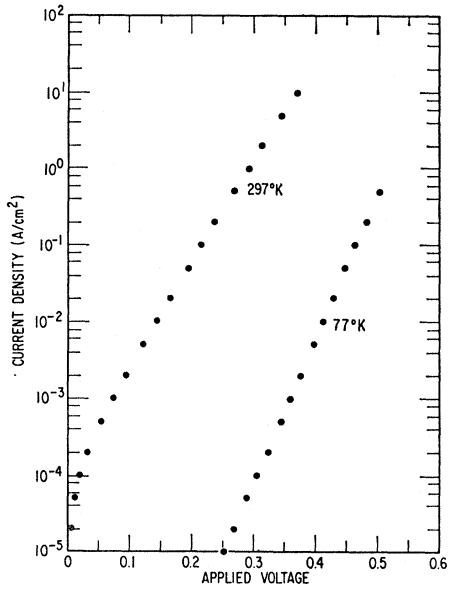

FIG. 11. Forward-current characteristic of a Sn-GaAs Schottky barrier at 77 and 297°K.

appropriate values from Table III, one achieves the same type of agreement with two-band field emission as was achieved with gold contacts. The room-temperature current behavior indicates that thermionic field emission is the predominant mechanism, as expected.

Tin contacts were also fabricated with both higher and lower carrier concentrations than the unit discussed above. As with gold contacts, tin contacts on lower-doped materials were difficult to analyze because of extraneous leakage effect. With more heavily doped specimens, it was difficult to determine the carrier concentration and barrier height. These problems are more serious here than with gold junctions because of the lower barrier height. The current-voltage character-

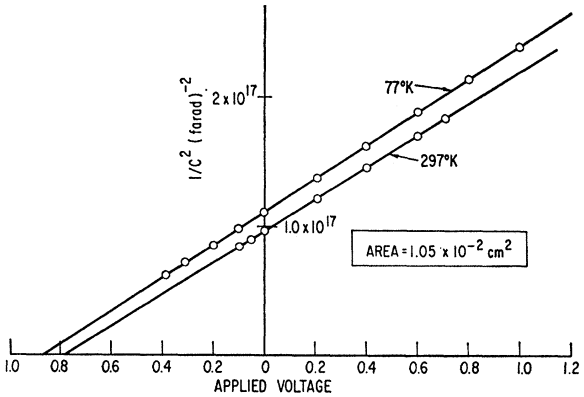

FIG. 12. Capacitance dependence of a Sn-GaAs contact at 77 and 297°K. This is the same unit whose forward-current behavior is presented in Fig. 11.

istics on more heavily doped GaAs follow the $\log_{10}J_0$-versus-S dependence expected from the measured tin-barrier energy.

Lead Schottky barriers have interesting characteristics but are not sufficiently stable to allow the type of analysis used with gold and tin contacts. Lead contacts are more difficult to fabricate than either gold or tin. The relatively high vapor pressure of lead permits reasonable evaporation rates at low evaporation temperatures. If lead contacts are formed at the same evaporation rate as gold or tin, a nonideal Schottky barrier results. Both the current-voltage and capacitance dependence suggest the presence of a thin interfacial layer between the lead and GaAs. By increasing the evaporation temperature, one can achieve ideal-type junctions. It is reasonable to suggest that a chemically polished surface has a weakly bonded interfacial layer that is stripped during evaporation if the evaporating atoms have sufficient energy.

When we fabricated lead contacts that initially displayed an ideal-type behavior, another interesting feature of lead contacts was observed. The barrier height decreased with time. Since no reasonable explanation for the instability of lead contacts could be offered, a detailed analysis of their characteristics is unjustified.

V. DISCUSSION

The present investigation indicates that the analysis of Padovani and Stratton for field emission in GaAs Schottky barriers is in excellent agreement with experimental results if one uses Franz's two-band model for the dispersion of states of the forbidden gap. This agreement is reached with the voltage dependence of semilog slope of the forward current and also the magnitude of forward current. Heretofore the magnitude of a forward current has received no experimental verification. Measurements of $d\ln J/dE$ versus E have been attempted in the past on GaAs but have disagreed in certain details with the above conclusion. Padovani and Stratton[10] deduced, from one Au-GaAs contact, a higher k_n^2 value than observed in this study. Conley and Mahan[11] examined several junctions that indicated a lower k_n^2 value than Padovani and Stratton, but there is a large amount of scatter in their results. It is reasonable to suggest that the discrepancy between the present and previous measurements of k_n^2 versus E does not present an intrinsic difficulty but can be related to the accuracy of the carrier-concentration determination. According to Eqs. (4) and (1i) and the carrier-concentration capacitance per unit area relationship, one can write

$$k_n^2 \propto S_m^{-2} \propto N \propto r^{-4},$$

where r is the radius for a circular contact. If one uses the carrier concentration determined from the Hall effect, a serious error is possible in determining k_n^2. Even if the carrier concentration is estimated from capacitance, the fourth-power dependence on diameter introduces an uncertainty unless well-defined contacts are used. Great care was taken in determining the areas of the contacts.

Chaves, Majlis, and Cardona[16] have calculated the imaginary electron wave number with the full-zone $\mathbf{k}\cdot\mathbf{p}$ method, and estimate that the dependence for the [111] direction should be nearly equal to the two-band model, but in the [110] direction it should be slightly larger. At 1.0 eV below the conduction band, k_n^2 in the [110] direction should be about 10% larger than in the [111]. There is no real difference between the [111] and [110] directions from the conduction band to 0.7 eV below. As previously stated, we have only observed that chemically polished surfaces [(111)], in general, exhibited slightly higher barrier energies than vacuum-cleaved samples [(110)], but in other respects gave identical results. The results on (111) and (110) surfaces obtained in this investigation do not allow us to make a valid judgment on the analysis by Chaves *et al.*, because of the experimental difficulties involved. Samples must have sufficiently large carrier concentrations to avoid leakage effects at low biases. Yet if the concentrations are to be calculated, the doping cannot be too heavy or capacitance measurements are not possible. These considerations limit the carrier concentrations to a very narrow range. Many attempts were made, but no concentrations in this range were encountered.

In closing, the authors call attention to the fact that the basic theoretical understanding to this work was laid over forty-five years ago by Wilson,[1] by Nordheim,[2] and by Frenkel and Joffé.[3] Their principal theoretical predictions have been observed in this work.

ACKNOWLEDGMENTS

The authors wish to thank M. Hellman for assistance during the preliminary phase of this work and E. L. Nealy and M. Edgren for technical assistance throughout this investigation. Many interesting and valuable discussions with Dr. F. Vernon, Jr., Dr. F. Padovani, and Dr. C. Crowell are gratefully acknowledged.